-ATG7 (Sigma Aldrich, A2856). FK506 (20% powder dissolved in water) for use in the animal studies was a gift from Astellas Pharma Inc. FK506 (Sigma-Aldrich, F4679) for use in the cell culture model assay was dissolved in dimethyl sulfoxide (DMSO; Sigma, D4540). Monodansylcadaverine (MDC; Sigma, 30432) was used for labeling autolysosomes and dissolved in ethanol (Nacalai, 14713-95).

Animal models. Four-week-old transgenic mice overexpressing hamster PRNP [Tg(Sha *Prnp*)], and CD-1 male mice (Charles River Laboratories International), were inoculated intracerebrally with 20 μl of brain homogenate from 263K-infected hamster and Fukuoka-1-infected mice, respectively. Mice were monitored weekly until the terminal stage of disease or until sacrificed. Clinical onset was defined as the presence of 3 or more of the following signs: greasy and/or yellowish hair, hunchback, weight loss, yellow pubes, ataxic gait and nonparallel hind limbs. Brains were removed, and the right hemispheres frozen and homogenized at 20% (w/v) in phosphate-buffered saline (PBS; Nacalai Tesque, 14249). Total proteins were extracted by mixing with the same amount of 2 × lysis buffer [1% Triton X-100 (Wako, 168-11085), 1% Deoxycholic acid (Wako, 046-18811), 300 mM NaCl (Nakalai, 31320-05), 50 mM Tris (Nakalai, 35434-2)-HCl (WAKO, 080-01066), pH 7.5].

In vivo administration of FK506. In Fukuoka 1-infected CD-1 mice, FK506 (1.0 or 0.1 mg/kg/day) was intraperitoneally administered from 20 or 60 d post-inoculation (d.p.i.). In 263K-infected Tg(Sha *Prnp*) mice, treatment with FK506 (1.0 mg/kg/day, orally) was started either from 14 d.p.i. or 28 d.p.i.

Cell culture. N2a58 and MG20 cells were prepared as described previously.[47,48] Fukuoka-1-infected N2a58 (N2a58/Fukuoka-1) and MG20 cells (MG20/Fukuoka-1) were produced by inoculation with brain homogenates harvested from Fukuoka-1-infected, terminally ill ddY mice. All cell media was supplemented with 10% fetal bovine serum and penicillin-streptomycin (Nacalai, 09367-34). Cells were incubated at 37°C and 5% CO_2, and sub-cultured every 3 to 4 d at a 5- to 10-fold dilution. N2a58 cells and N2a58/Fukuoka-1 cells were cultured in high-glucose Dulbecco's modified Eagle's medium (DMEM; Wako Pure Chemical Industries, 043-30085) and Opti-MEM (Gibco-Invitrogen, 31985), respectively. MG20 and MG20/Fukuoka-1 cells were cultured in low-glucose DMEM (Wako, 041-29775) supplemented with 10 μM 2-mercaptoethanol (Sigma, M3148) and 10 μg/ml insulin (Sigma, I3536). Both N2a58/Fukuoka-1 and MG20/Fukuoka-1 cells stably produced $PRNP^{Sc}$ for over 30 passages.

FK506 treatment in cell cultures. Cells (3.5×10^5 cells/well) were grown in 6-well plates for 24 h prior to the addition of different concentrations of FK506 diluted in the same volume of DMSO. As a negative control, DMSO alone was used. After treatment for 48 h, the proteins were collected in lysis buffer (0.5% Triton X-100, 0.5% Deoxycholic acid, 150 mM NaCl and 50 mM TRIS-HCl, PH 7.5) and analyzed by western blotting. To inhibit lysosomal activity, cells were initially treated with 10 mM of NH_4Cl (Wako, 017-02995) for 24 h, after which 30 μM of FK506 was added and the cells were cultured for a further 24 h.

MDC assay. Cells were treated with 10 μM of FK506 for 24 h or HBSS for 30 min, and then incubated with 0.1 mM of MDC in PBS for 30 min at 37°C. The cells were then washed with PBS twice and observed using an Axio Observer Z1 (Carl Zeiss, 431007-9901). The granules of MDC were counted using an INCell Analyzer 1000 (GE Healthcare, 25-8010-26).

Western blotting. Total protein concentrations were measured using a BCA protein assay kit (Pierce, 23227). To detect $PRNP^{Sc}$, the samples were digested with PK (40 μg/mg protein) for 30 min at 37°C. Loading buffer [50 mM TRIS-HCl (pH 6.8), containing 5% glycerol (Kanto Chemical, 17029-00), 1.6% SDS (Nakalai, 31606-75) and 100 mM dithiothreitol (Nakalai, 14128-62)] was added to the proteins, and the mixtures incubated at 95°C for 10 min. SDS-PAGE was performed using 15% acrylamide gels. The proteins were transferred onto an Immobilon-P membrane (Millipore, IPVH10100) in a transfer buffer containing 20% methanol, and the membrane was blocked with 5% nonfat dry milk in TBST [10 mM TRIS-HCl (pH 7.8), 100 mM NaCl, 0.1% Tween 20 (Wako, 591-09825)] for 60 min at room temperature and reacted with primary antibody overnight at 4°C. Immunoreactive bands were visualized using the enhanced ECL plus chemiluminescence system (GE Healthcare, RPN2132).

Histochemistry. The brain tissues were fixed in 10% neutral buffered formalin (Wako, 066-03847). The fixed hemispheres were embedded in paraffin and sectioned into 3 μm slices. To evaluate the spongiform change, the tissue sections were stained with hematoxylin (Wako, 131-09665) and eosin (Wako, 056-06722). For AIF1 and GFAP staining, after deparaffinization and rehydration, the sections were treated with 0.3% hydrogen peroxidase (Wako, 086-07445) in methanol (Hayashi Pure Chemical, 130-02069) for 30 min to inactivate endogenous peroxidase and then incubated with 3% nonfat dry milk (Megmilk Snow Brand, FA-08) in TBST for 60 min at room temperature. The blocked sections were reacted with primary antibody overnight at room temperature, then reacted with envision polymer horseradish peroxidase (HRP)-conjugated anti-rabbit immunoglobulin G antibodies (Dako, K4002) for 60 min at room temperature. Immunostaining was visualized using 3, 3-diaminobenzidine (DAB; Dojindo Lab, D006). The hydrolytic autoclaving and formic acid method for $PRNP^{Sc}$ staining has been described previously.[49]

Statistical analysis. The unpaired t-test or Welch's correction was used for comparison between the two groups. For multiple comparison the one-way ANOVA followed by the Tukey-Kramer test was used. The log rank test was used for analyzing the survival time of prion-infected mice. All statistical analysis was performed using GraphPad Prism software.

Disclosure of Potential Conflicts of Interest

No potential conflicts of interest were disclosed.

Acknowledgments

We thank Dr. Hitoki Yamanaka for helpful discussions, and Mari Kudo, Atsuko Matsuo and Ayumi Yamakawa for technical assistance. This work was supported by the Global Centers of Excellence Program (F12); a grant-in-aid for science research (B;

grant no. 23300127) from the Ministry of Education, Culture, Sports, Science and Technology of Japan; a grant for bovine spongiform encephalopathy research and a grant-in-aid from the Research Committee of Prion disease and Slow Virus Infection, from the Ministry of Health, Labor and Welfare of Japan; a grant from Takeda Science Foundation.

Supplemental Materials

Supplemental materials may be found here:
www.landesbioscience.com/journals/autophagy/article/25381

References

1. Prusiner SB. Prions. Proc Natl Acad Sci U S A 1998; 95:13363-83; PMID:9811807; http://dx.doi.org/10.1073/pnas.95.23.13363
2. Aguzzi A, Polymenidou M. Mammalian prion biology: one century of evolving concepts. Cell 2004; 116:313-27; PMID:14744440; http://dx.doi.org/10.1016/S0092-8674(03)01031-6
3. Caughey B, Raymond GJ. Sulfated polyanion inhibition of scrapie-associated PrP accumulation in cultured cells. J Virol 1993; 67:643-50; PMID:7678300
4. Doh-Ura K, Iwaki T, Caughey B. Lysosomotropic agents and cysteine protease inhibitors inhibit scrapie-associated prion protein accumulation. J Virol 2000; 74:4894-7; PMID:10775631; http://dx.doi.org/10.1128/JVI.74.10.4894-4897.2000
5. White AR, Enever P, Tayebi M, Mushens R, Linehan J, Brandner S, et al. Monoclonal antibodies inhibit prion replication and delay the development of prion disease. Nature 2003; 422:80-3; PMID:12621436; http://dx.doi.org/10.1038/nature01457
6. Ishibashi D, Yamanaka H, Mori T, Yamaguchi N, Yamaguchi Y, Nishida N, et al. Antigenic mimicry-mediated anti-prion effects induced by bacterial enzyme succinylarginine dihydrolase in mice. Vaccine 2011; 29:9321-8; PMID:22008817; http://dx.doi.org/10.1016/j.vaccine.2011.10.017
7. Cashman NR, Caughey B. Prion diseases--close to effective therapy? Nat Rev Drug Discov 2004; 3:874-84; PMID:15459678; http://dx.doi.org/10.1038/nrd1525
8. Brazier MW, Volitakis I, Kvasnicka M, White AR, Underwood JR, Green JE, et al. Manganese chelation therapy extends survival in a mouse model of M1000 prion disease. J Neurochem 2010; 114:440-51; PMID:20456001; http://dx.doi.org/10.1111/j.1471-4159.2010.06771.x
9. Tsuboi Y, Doh-Ura K, Yamada T. Continuous intraventricular infusion of pentosan polysulfate: clinical trial against prion diseases. Neuropathology 2009; 29:632-6; PMID:19788637; http://dx.doi.org/10.1111/j.1440-1789.2009.01058.x
10. Collinge J, Gorham M, Hudson F, Kennedy A, Keogh G, Pal S, et al. Safety and efficacy of quinacrine in human prion disease (PRION-1 study): a patient-preference trial. Lancet Neurol 2009; 8:334-44; PMID:19278902; http://dx.doi.org/10.1016/S1474-4422(09)70049-3
11. Zerr I. Therapeutic trials in human transmissible spongiform encephalo-pathies: recent advances and problems to address. Infect Disord Drug Targets 2009; 9:92-9; PMID:19200019; http://dx.doi.org/10.2174/1871526510909010092
12. Brazier MW, Wall VA, Brazier BW, Masters CL, Collins SJ. Therapeutic interventions ameliorating prion disease. Expert Rev Anti Infect Ther 2009; 7:83-105; PMID:19622059; http://dx.doi.org/10.1586/14787210.7.1.83
13. Mizushima N, Levine B, Cuervo AM, Klionsky DJ. Autophagy fights disease through cellular self-digestion. Nature 2008; 451:1069-75; PMID:18305538; http://dx.doi.org/10.1038/nature06639
14. Cheung ZH, Ip NY. Autophagy deregulation in neurodegenerative diseases - recent advances and future perspectives. J Neurochem 2011; 118:317-25; PMID:21599666; http://dx.doi.org/10.1111/j.1471-4159.2011.07314.x
15. Williams A, Sarkar S, Cuddon P, Ttofi EK, Saiki S, Siddiqi FH, et al. Novel targets for Huntington's disease in an mTOR-independent autophagy pathway. Nat Chem Biol 2008; 4:295-305; PMID:18391949; http://dx.doi.org/10.1038/nchembio.79
16. Schaeffer V, Lavenir I, Ozcelik S, Tolnay M, Winkler DT, Goedert M. Stimulation of autophagy reduces neurodegeneration in a mouse model of human tauopathy. Brain 2012; 135:2169-77; PMID:22689910; http://dx.doi.org/10.1093/brain/aws143
17. Aguib Y, Heiseke A, Gilch S, Riemer C, Baier M, Schätzl HM, et al. Autophagy induction by trehalose counteracts cellular prion infection. Autophagy 2009; 5:361-9; PMID:19182537; http://dx.doi.org/10.4161/auto.5.3.7662
18. Heiseke A, Aguib Y, Riemer C, Baier M, Schätzl HM. Lithium induces clearance of protease resistant prion protein in prion-infected cells by induction of autophagy. J Neurochem 2009; 109:25-34; PMID:19183256; http://dx.doi.org/10.1111/j.1471-4159.2009.05906.x
19. Cortes CJ, Qin K, Cook J, Solanki A, Mastrianni JA. Rapamycin delays disease onset and prevents PrP plaque deposition in a mouse model of Gerstmann-Sträussler-Scheinker disease. J Neurosci 2012; 32:12396-405; PMID:22956830; http://dx.doi.org/10.1523/JNEUROSCI.6189-11.2012
20. Bové J, Martínez-Vicente M, Vila M. Fighting neurodegeneration with rapamycin: mechanistic insights. Nat Rev Neurosci 2011; 12:437-52; PMID:21772323; http://dx.doi.org/10.1038/nrn3068
21. Kaminska B, Gaweda-Walerych K, Zawadzka M. Molecular mechanisms of neuroprotective action of immunosuppressants--facts and hypotheses. J Cell Mol Med 2004; 8:45-58; PMID:15090260; http://dx.doi.org/10.1111/j.1582-4934.2004.tb00259.x
22. Brecht S, Waetzig V, Hidding U, Hanisch UK, Walther M, Herdegen T, et al. FK506 protects against various immune responses and secondary degeneration following cerebral ischemia. Anat Rec (Hoboken) 2009; 292:1993-2001; PMID:19728359; http://dx.doi.org/10.1002/ar.20994
23. Yoshiyama Y, Higuchi M, Zhang B, Huang SM, Iwata N, Saido TC, et al. Synapse loss and microglial activation precede tangles in a P301S tauopathy mouse model. Neuron 2007; 53:337-51; PMID:17270732; http://dx.doi.org/10.1016/j.neuron.2007.01.010
24. Gerard M, Deleersnijder A, Daniëls V, Schreurs S, Munck S, Reumers V, et al. Inhibition of FK506 binding proteins reduces α-synuclein aggregation and Parkinson's disease-like pathology. J Neurosci 2010; 30:2454-63; PMID:20164329; http://dx.doi.org/10.1523/JNEUROSCI.5983-09.2010
25. Mukherjee A, Morales-Scheihing D, Gonzalez-Romero D, Green K, Taglialatela G, Soto C. Calcineurin inhibition at the clinical phase of prion disease reduces neurodegeneration, improves behavioral alterations and increases animal survival. PLoS Pathog 2010; 6:e1001138; PMID:20949081; http://dx.doi.org/10.1371/journal.ppat.1001138
26. Juhász G, Puskás LG, Komonyi O, Erdi B, Maróy P, Neufeld TP, et al. Gene expression profiling identifies FKBP39 as an inhibitor of autophagy in larval Drosophila fat body. Cell Death Differ 2007; 14:1181-90; PMID:17363962; http://dx.doi.org/10.1038/sj.cdd.4402123
27. Schuck P. Reliable determination of binding affinity and kinetics using surface plasmon resonance biosensors. Curr Opin Biotechnol 1997; 8:498-502; PMID:9265731; http://dx.doi.org/10.1016/S0958-1669(97)80074-2
28. Kuwata K, Nishida N, Matsumoto T, Kamatari YO, Hosokawa-Muto J, Kodama K, et al. Hot spots in prion protein for pathogenic conversion. Proc Natl Acad Sci U S A 2007; 104:11921-6; PMID:17616582; http://dx.doi.org/10.1073/pnas.0702671104
29. Tanida I. Autophagosome formation and molecular mechanism of autophagy. Antioxid Redox Signal 2011; 14:2201-14; PMID:20712405; http://dx.doi.org/10.1089/ars.2010.3482
30. Munafó DB, Colombo MI. A novel assay to study autophagy: regulation of autophagosome vacuole size by amino acid deprivation. J Cell Sci 2001; 114:3619-29; PMID:11707514
31. Amenta JS, Hlivko TJ, McBee AG, Shinozuka H, Brocher S. Specific inhibition by NH4CL of autophagy-associated proteloysis in cultured fibroblasts. Exp Cell Res 1978; 115:357-66; PMID:689091; http://dx.doi.org/10.1016/0014-4827(78)90289-6
32. Scott M, Foster D, Mirenda C, Serban D, Coufal F, Wälchli M, et al. Transgenic mice expressing hamster prion protein produce species-specific scrapie infectivity and amyloid plaques. Cell 1989; 59:847-57; PMID:2574076; http://dx.doi.org/10.1016/0092-8674(89)90608-9
33. Imai Y, Ibata I, Ito D, Ohsawa K, Kohsaka S. A novel gene iba1 in the major histocompatibility complex class III region encoding an EF hand protein expressed in a monocytic lineage. Biochem Biophys Res Commun 1996; 224:855-62; PMID:8713135; http://dx.doi.org/10.1006/bbrc.1996.1112
34. Ito D, Imai Y, Ohsawa K, Nakajima K, Fukuuchi Y, Kohsaka S. Microglia-specific localisation of a novel calcium binding protein, Iba1. Brain Res Mol Brain Res 1998; 57:1-9; PMID:9630473; http://dx.doi.org/10.1016/S0169-328X(98)00040-0
35. Ma J, Lindquist S. Wild-type PrP and a mutant associated with prion disease are subject to retrograde transport and proteasome degradation. Proc Natl Acad Sci U S A 2001; 98:14955-60; PMID:11742063; http://dx.doi.org/10.1073/pnas.011578098
36. Yedidia Y, Horonchik L, Tzaban S, Yanai A, Taraboulos A. Proteasomes and ubiquitin are involved in the turnover of the wild-type prion protein. EMBO J 2001; 20:5383-91; PMID:11574470; http://dx.doi.org/10.1093/emboj/20.19.5383
37. Kristiansen M, Deriziotis P, Dimcheff DE, Jackson GS, Ovaa H, Naumann H, et al. Disease-associated prion protein oligomers inhibit the 26S proteasome. Mol Cell 2007; 26:175-88; PMID:17466621; http://dx.doi.org/10.1016/j.molcel.2007.04.001
38. Deriziotis P, André R, Smith DM, Goold R, Kinghorn KJ, Kristiansen M, et al. Misfolded PrP impairs the UPS by interaction with the 20S proteasome and inhibition of substrate entry. EMBO J 2011; 30:3065-77; PMID:21743439; http://dx.doi.org/10.1038/emboj.2011.224
39. Aguzzi A, Heikenwalder M. Pathogenesis of prion diseases: current status and future outlook. Nat Rev Microbiol 2006; 4:765-75; PMID:16980938; http://dx.doi.org/10.1038/nrmicro1492

40. Forloni G, Angeretti N, Chiesa R, Monzani E, Salmona M, Bugiani O, et al. Neurotoxicity of a prion protein fragment. Nature 1993; 362:543-6; PMID:8464494; http://dx.doi.org/10.1038/362543a0
41. Rock RB, Gekker G, Hu S, Sheng WS, Cheeran M, Lokensgard JR, et al. Role of microglia in central nervous system infections. Clin Microbiol Rev 2004; 17:942-64; PMID:15489356; http://dx.doi.org/10.1128/CMR.17.4.942-964.2004
42. Falsig J, Julius C, Margalith I, Schwarz P, Heppner FL, Aguzzi A. A versatile prion replication assay in organotypic brain slices. Nat Neurosci 2008; 11:109-17; PMID:18066056; http://dx.doi.org/10.1038/nn2028
43. Kranich J, Krautler NJ, Falsig J, Ballmer B, Li S, Hutter G, et al. Engulfment of cerebral apoptotic bodies controls the course of prion disease in a mouse strain-dependent manner. J Exp Med 2010; 207:2271-81; PMID:20837697; http://dx.doi.org/10.1084/jem.20092401
44. Tanaka K, Asanuma M, Ogawa N. Molecular basis of anti-apoptotic effect of immunophilin ligands on hydrogen peroxide-induced apoptosis in human glioma cells. Neurochem Res 2004; 29:1529-36; PMID:15260130; http://dx.doi.org/10.1023/B:NERE.0000029565.92587.25
45. Hampe J, Franke A, Rosenstiel P, Till A, Teuber M, Huse K, et al. A genome-wide association scan of nonsynonymous SNPs identifies a susceptibility variant for Crohn disease in ATG16L1. Nat Genet 2007; 39:207-11; PMID:17200669; http://dx.doi.org/10.1038/ng1954
46. Rioux JD, Xavier RJ, Taylor KD, Silverberg MS, Goyette P, Huett A, et al. Genome-wide association study identifies new susceptibility loci for Crohn disease and implicates autophagy in disease pathogenesis. Nat Genet 2007; 39:596-604; PMID:17435756; http://dx.doi.org/10.1038/ng2032
47. Nishida N, Harris DA, Vilette D, Laude H, Frobert Y, Grassi J, et al. Successful transmission of three mouse-adapted scrapie strains to murine neuroblastoma cell lines overexpressing wild-type mouse prion protein. J Virol 2000; 74:320-5; PMID:10590120; http://dx.doi.org/10.1128/JVI.74.1.320-325.2000
48. Iwamaru Y, Takenouchi T, Ogihara K, Hoshino M, Takata M, Imamura M, et al. Microglial cell line established from prion protein-overexpressing mice is susceptible to various murine prion strains. J Virol 2007; 81:1524-7; PMID:17121794; http://dx.doi.org/10.1128/JVI.01379-06
49. Ishibashi D, Atarashi R, Fuse T, Nakagaki T, Yamaguchi N, Satoh K, et al. Protective role of interferon regulatory factor 3-mediated signaling against prion infection. J Virol 2012; 86:4947-55; PMID:22379081; http://dx.doi.org/10.1128/JVI.06326-11

ChemPubSoc Europe

DOI: 10.1002/cmdc.201300167

Synthesis of an ^{11}C-Labeled Antiprion GN8 Derivative and Evaluation of Its Brain Uptake by Positron Emission Tomography

Tsutomu Kimura,[a] Takeo Sako,[b] Siqin,[b] Junji Hosokawa-Muto,[a] Yi Long Cui,[b] Yasuhiro Wada,[b] Yosky Kataoka,[b] Hisashi Doi,[b] Suehiro Sakaguchi,[c] Masaaki Suzuki,[b] Yasuyoshi Watanabe,[b] and Kazuo Kuwata*[a]

N,N'-(Methylenedi-4,1-phenylene)bis[2-(1-pyrrolidinyl) acetamide] (GN8) is a promising candidate for the treatment of prion diseases. The purpose of this study was to synthesize a GN8 derivative labeled with a positron emitting radionuclide and to clarify the blood–brain barrier (BBB) permeability of the resultant derivative by positron emission tomography (PET). As a key synthetic intermediate, a GN8 derivative bearing a tributylstannyl group was prepared from commercially available materials in four steps. Palladium(0)-mediated rapid C-methylation of the aryltributylstannane using [^{11}C]methyl iodide yielded a [^{11}C]methyl-substituted GN8 derivative ([^{11}C]-**1**) with sufficient radioactivity (0.5–2.0 GBq) and specific radioactivity in the region of 60–126 GBq μmol^{-1}. [^{11}C]-**1** was injected into the tail vein of rats, and its biodistribution was determined by PET; the results unambiguously demonstrated the brain penetration of [^{11}C]-**1** in rat brain.

Prion diseases, also referred to as transmissible spongiform encephalopathies (TSEs), are a family of fatal neurodegenerative disorders that affect both humans and animals.[1,2] Human prion diseases include Creutzfeldt–Jakob disease (CJD), Gerstmann–Sträussler–Scheinker (GSS) syndrome, fatal familial insomnia, and kuru. The representatives of animal prion diseases are scrapie in sheep and goats, bovine spongiform encephalopathy (BSE) in cattle, and chronic wasting disease in deer and elk. These disorders are characterized by vacuolar degeneration of the central nervous system (CNS). The causative agent of the diseases is thought to be an infectious isoform of the prion protein, designated PrP^{Sc}, and an accumulation of PrP^{Sc} in the CNS gives rise to prion diseases.

Since the epidemic of BSE and the appearance of a new variant of CJD, which seems to be caused by PrP^{Sc}-contaminated beef consumption, much effort has been devoted to developing a therapeutic agent for prion diseases. A wide range of compounds have been identified as having antiprion activity in TSE-infected cells.[3,4] However, current therapeutic agents directed at prion diseases remain unsatisfactory[5,6] due to a lack of blood–brain barrier (BBB) permeability. Although an intraventricular injection of BBB-impermeable antiprion compounds is an alternative route for drug administration, it is invasive and harmful to the patients, and poses a risk for iatrogenic prion infections. Therefore, it is essential to develop antiprion agents that can cross the BBB.

During the course of our antiprion drug discovery and development studies,[7,8] GN8 was identified as a novel antiprion compound (Figure 1 a).[9–15] Subcutaneous administration of GN8 offered a survival benefit to TSE-infected mice.[9] Furthermore, nonclinical safety assessment of GN8 in rats and dogs revealed that GN8 could be used safely at the concentration nec-

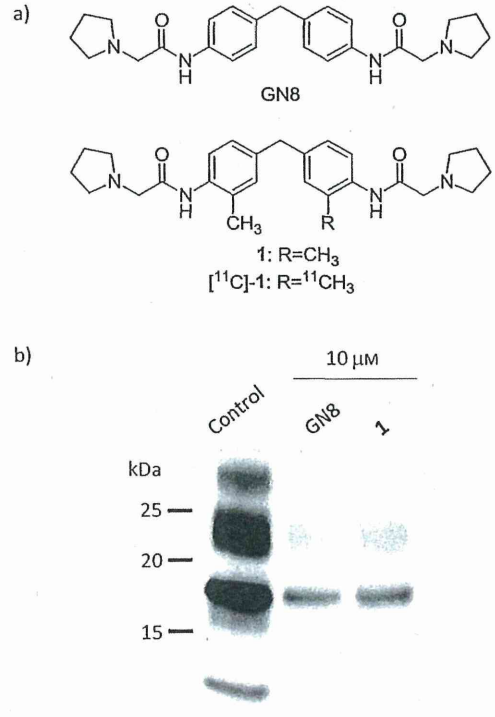

Figure 1. a) Chemical structures of GN8, and the unlabeled and ^{11}C-labeled methylated derivative of GN8 (**1**). b) Western blotting of proteinase K-resistant prion protein in GT+FK cells after treatment of the cells with GN8 and **1** at 10 μM.

[a] *Dr. T. Kimura, Dr. J. Hosokawa-Muto, Prof. K. Kuwata*
Center for Emerging Infectious Diseases
United Graduate School of Drug Discovery & Medical Information Sciences
Gifu University, 1-1 Yanagido, Gifu 501-1194 (Japan)
E-mail: kuwata@gifu-u.ac.jp

[b] *Dr. T. Sako, Dr. Siqin, Dr. Y. L. Cui, Dr. Y. Wada, Dr. Y. Kataoka, Dr. H. Doi, Prof. M. Suzuki, Prof. Y. Watanabe*
RIKEN Center for Molecular Imaging Science
6-7-3 Minatojima, Minamimachi, Chuo-ku, Kobe, Hyogo 650-0047 (Japan)

[c] *Prof. S. Sakaguchi*
Institute for Enzyme Research, Tokushima University
3-18-15 Kuramoto-cyo, Tokushima, 770-8503 (Japan)

Supporting information for this article is available on the WWW under http://dx.doi.org/10.1002/cmdc.201300167.

essary to exert antiprion activity.[15] PET is a powerful technique to assess the clinical dose, regimen selection, as well as brain penetration of the emitter-labeled compounds in prion disease patients. PET analysis of a GN8 derivative labeled with a positron-emitting radionuclide would give us important clues for antiprion drug development.[16] Herein, we report the synthesis of a ^{11}C-labeled GN8 derivative ([^{11}C]-**1**) by palladium-catalyzed rapid methylation of aryltributylstannane, and its subsequent assessment for BBB permeability and biodistribution in rat by PET.

As a positron emitting radionuclide-labeled compound, we designed [^{11}C]-**1** in which two methyl groups are linked to the diphenylmethane unit of GN8 at the 2,2'-positions via carbon–carbon bonds (Figure 1a). To confirm the antiprion activity of the dimethyl-modified GN8 derivative, cold GN8 derivative **1** was prepared by bromoacetylation of 4,4'-diamino-3,3'-dimethyldiphenylmethane and subsequent substitution of the bromo groups with pyrrolidine (see Supporting Information).[14] The antiprion activity of **1** was tested in GT+FK cells, which are mouse neuronal cells (GT1–7) persistently infected with a mouse-adapted GSS agent (Fukuoka-1 strain) (Figure 1b).[7,17,18] GN8 derivative **1** exhibited a similar order of activity to that of GN8 with an IC_{50} value of 2.35±0.12 μM. Thus, the modification of GN8 by the introduction of two methyl groups did not substantially affect its antiprion activity.[9]

^{11}C is a short-lived positron emitting radionuclide ($t_{1/2}$= 20.4 min). A ^{11}C-labeled methyl group can be incorporated into an aromatic framework via a carbon–carbon bond in a short synthesis time using palladium(0)-mediated rapid cross-coupling of aryltributylstannane with [^{11}C]methyl iodide.[19–23] Aryltributylstannane **4** is a key synthetic intermediate for the synthesis of [^{11}C]-**1** by rapid C-[^{11}C]methylation (Scheme 1a). Initially, synthesis of **4** was examined via palladium-catalyzed tributylstannylation of aryl iodide **3**.[24] Unsymmetrically substituted 4,4'-diaminodiphenylmethane **2** was prepared from *ortho*-toluidine, 2-iodoaniline hydrochloride, and paraformaldehyde.[14,25] Bromoacetylation of diamine **2** and subsequent substitution reaction of the resulting bis(2-bromoacetamide) with pyrrolidine yielded compound **3**.[14] Unfortunately, several attempts to convert **3** to **4** by palladium-catalyzed tributylstannylation with bis(tributylstannane) were unsuccessful, presumably because of the substituent effect of the neighboring acylamino group. Alternatively, we examined the synthesis of **4** via tributylstannylation at an earlier stage. Aryl iodide **2** underwent a palladium-catalyzed coupling reaction with bis(tributylstannane) to afford aryltributylstannane **5** at a yield of 67%. Chloroacetylation of **5** gave bis(2-chloroacetamide) **6**, and the reaction of **6** with pyrrolidine in the presence of K_2CO_3 provided the desired aryltributylstannane **4**.

With the key precursor in hand, rapid methylation of aryltributylstannane **4** with [^{11}C]methyl iodide was carried out in the presence of palladium catalyst (Scheme 1b).[19–23] After several experiments, we found that *N*-methylpyrrolidone (NMP) was an effective solvent for the rapid methylation of aryltributylstannane **4**. The optimized conditions for the reaction of aryltributylstannane **4** with [^{11}C]methyl iodide were NMP for five minutes to give the ^{11}C-labeled GN8 derivative [^{11}C]-**1** with sufficient radioactivity (0.5–2.0 GBq) for PET and a specific radioactivity of 60–126 GBq μmol^{-1}. The chemical purity analyzed at 254 nm was 82–92%, and the radiochemical purity was determined to be greater than 95%. The decay-corrected radiochemical yield, which was calculated from the radioactivity of [^{11}C]methyl iodide trapped in the palladium catalyst-containing reaction mixture, was approximately 20%. The total synthesis time, including HPLC purification and radiopharmaceutical formulation for intravenous administration, was 43 min.

To investigate the BBB permeability and the biodistribution of [^{11}C]-**1**, consecutive PET scans of the brain and whole body of Sprague–Dawley rats (n=4) were conducted. A 90 minute emission scan of the brain revealed that, after intravenous ad-

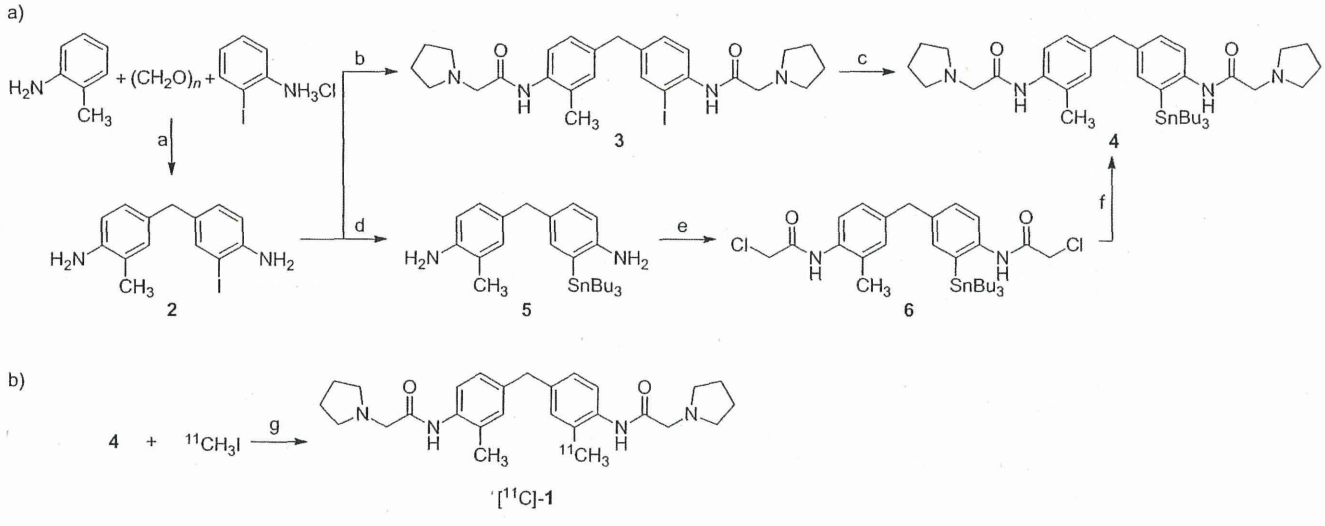

Scheme 1. Synthesis of aryltributylstannane **4** and radiosynthesis of ^{11}C-labeled GN8 derivative [^{11}C]-**1** by palladium-catalyzed rapid methylation with [^{11}C]-CH_3I. *Reagents and conditions*: a) CH_3OH, reflux, 18 h, 22%; b) 1. $BrCH_2C(O)Br$, pyridine, DMAP, CH_2Cl_2, 25 °C, 3 h; 2. pyrrolidine, K_2CO_3, THF, 60 °C, 12 h, 69% (two steps); c) $(Bu_3Sn)_2$, $Pd(PPh_3)_4$ (10 mol%), toluene, reflux, 48 h, 10%; d) $(Bu_3Sn)_2$, $Pd(PPh_3)_4$ (5 mol%), toluene, 100 °C, 24 h, 67%; e) $ClCH_2C(O)Cl$, Et_3N, CH_2Cl_2, 0 °C, 10 min, 83%; f) pyrrolidine, K_2CO_3, THF, 60 °C, 12 h, 92%; g) $Pd_2(dba)_3$, (*o*-tolyl)$_3$P, CuCl, K_2CO_3, NMP, 80 °C, 5 min.

ministration of [^{11}C]-**1**, radioactivity was observed in the pituitary gland, pineal body, cerebral cortex, and choroid plexus (Figure 2a). Around the head and neck, accumulation of [^{11}C]-**1** was observed in the thyroid gland, submandibular gland, and Harderian gland (Figure 2a). Whole-body PET images indicated that [^{11}C]-**1** uptake was scanned in the lung, liver, kidney, intestine, and spleen (Figure 2b). After the PET scan, the

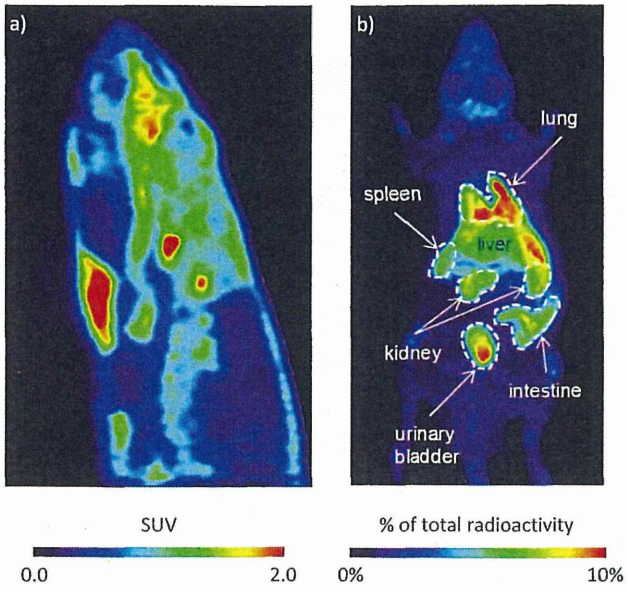

Figure 2. Positron emission tomography (PET) images of the brain and whole body. a) Maximum a posteriori probability (MAP) algorithm reconstructed static image taken 5–90 min after [^{11}C]-**1** injection (sagittal). b) Maximum intensity projection (MIP) image of 90–120 min after [^{11}C]-**1** injection. Standardized uptake values (SUV) are a semi-quantitative measure, derived from determination of tissue activity obtained from a single static image.

organs of the animal were dissected and the radioactivity of each tissue was measured with a gamma counter.

The tissue distribution data were in good agreement with the PET images, and the radioactivity of the brain was found to be higher than that of the blood or muscle (Table 1). These results demonstrated that [^{11}C]-**1** administered intravenously crosses the BBB and is retained in the brain.

To evaluate the degradation of **1** in vivo, we monitored its intravenous as well as intrabrain concentration in a time-dependent manner using a gas chromatography–mass spectrometry (GC/MS). The results showed that the elimination half-life of **1** is much longer than 24 hours, indicating that radioactivity is not originated from the degraded [^{11}C]-**1** (data not shown).

To confirm the distribution in brain, [^{11}C]-**1** was injected into rats, which were then sacrificed 40 minutes after administration. Auto-radiographic images of coronal sections of rat brain at 60 minutes post-injection are shown in Figure 3 along with their photographs. The auto-radiographic images clearly demonstrated that [11C]-**1** is primarily localized in the cerebral cortex, pineal body, pituitary gland, and choroid plexus.

Introduction of ^{11}C-lableled methyl group through a carbon–carbon bond is fascinating because it is resistant to in vivo metabolism in marked contrast to carbon–heteroatom bonds.

Table 1. Biodistribution data for [^{11}C]-**1**.

Tissue	ID [%][a]
Lung	4.98 ± 0.08
Kidney	2.17 ± 0.11
Spleen	2.11 ± 0.11
Liver	1.21 ± 0.06
Brain	0.36 ± 0.01
Heart	0.23 ± 0.03
Muscle	0.093 ± 0.005
Fat	0.04 ± 0.02
Blood	0.03 ± 0.002

[a] Data are the percent injected dose per gram of tissue ± standard error of the mean (SEM) of $n = 4$ independent experiments.

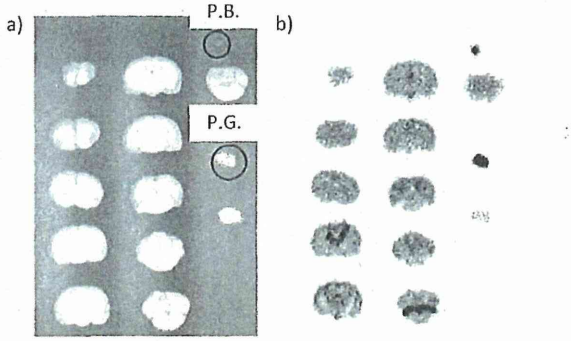

Figure 3. a) Photographic images of coronal sections of rat brain, and b) the corresponding auto-radiographic images at 60 min postinjection of [^{11}C]-**1**. Abbreviations: pineal body (P.B.) and pituitary gland (P.G.).

Transition-metal-catalyzed cross-coupling reactions are useful methods for constructing carbon–carbon bonds with excellent functional group tolerance.[26] We adopted palladium(0)-mediated rapid C-[^{11}C]-methylation using arylstannane **4** and [^{11}C]methyl iodide as a ^{11}C-labeling method,[19–23] since the conventional palladium-catalyzed cross-coupling reaction generally takes several hours. In addition, in practical terms, the ^{11}C-labeling must typically be carried out with small quantities of [^{11}C]methyl iodide (less than micromolar amounts) and excess amounts of stannyl precursor (greater than micromolar amounts). Thus, the palladium(0)-mediated rapid C-[^{11}C]methylation is an efficient method for ^{11}C-labeling that can meet the chemically difficult demands of radiolabeling conditions.[27,28]

As mentioned above, to date, a variety of compounds have already been identified as antiprion compounds in TSE-infected cells.[3,4] However, most of these compounds were ineffective in vivo, and only a limited number of compounds including amphotericin B and its derivative, pentosan polysulfate, and porphyrin derivatives have been reported to be effective in TSE-infected animals.[29–31] In clinical trials, pentosan polysulfate had to be administered intraventricularly since it did not penetrate the BBB, and no apparent improvement of clinical features was observed in the patients treated with this agent.[32] Treatment with quinacrine also failed to provide a therapeutic benefit, rather, it led to liver dysfunction.[33–35]

These agents were originally developed for the treatment of interstitial cystitis and malaria, respectively, and would not be suitable for the treatment of CNS disorders. Therefore, the pharmacokinetic properties, especially the BBB permeability, of the compounds should be carefully considered in drug development for prion diseases.[36,37] Previously, we reported that the subcutaneous administration of GN8 prolonged the lifetime of prion-infected mice, indicating that GN8 can enter the brain across the BBB. In this study, we confirmed that [^{11}C]-**1** administered intravenously also reaches the brain.

In summary, an ^{11}C-labeled GN8 derivative [^{11}C]-**1**, in which an ^{11}C-labeled methyl group was connected to the aromatic ring via a carbon–carbon bond, was successfully synthesized by palladium-catalyzed rapid methylation of aryl-(tributyl)stannane with [^{11}C]methyl iodide. PET analysis using the ^{11}C-labeled compound unequivocally demonstrated that the GN8 derivative penetrated into the brain. These findings will facilitate further refinement of GN8 as a therapeutic agent for prion diseases. Further studies on the application of the ^{11}C-labeled GN8 derivative as a molecular imaging probe for detecting cellular prion protein[38–40] in vivo are currently ongoing and will be reported in due course.

Experimental Section

PET studies using rats: Male Sprague–Dawley rats (Japan SLC, Inc., Hamamatsu, Shizuoka, Japan) at 8–9 weeks old and weighing approximately 250 g each were used in the study. All PET scans were performed using microPET F220 (Siemens Co., Ltd, Knoxville, TN, USA). Rats ($n=4$) were anesthetized and maintained with a mixture of 1.5% isoflurane and nitrous oxide/oxygen (7:3) and positioned in the PET scanner gantry. After intravenous bolus injection of [^{11}C]-**1** via the tail vein (~100 MBq per animal), a 90 min emission scan of the brain was performed with 400–650 keV as the energy window and 6 ns as the coincidence time window. Emission data of the brain were acquired in the list mode and sorted into dynamic sinograms (6×10 s, 6×30 s, 11×60 s, 15×180 s, 3×600 s; a total of 41 frames). After scanning the brain, a 30 min whole-body PET scan was conducted. For whole-body scans, the scanner bed was moved continuously in a reciprocating motion to ensure the entire body was scanned, and the list-mode data were sorted into dynamic sinogram for every one-bed pass. The data were reconstructed by a statistical maximum a posteriori probability algorithm (MAP) of ten iterations with point spread function (PSF) effect. During the experiment, a thermo-sensing probe was inserted into the rectum to monitor body temperature, which was maintained at 37 °C with a temperature controller (CMA150, CMA/Microdialysis, Stockholm, Sweden). The radioactivity concentrations were normalized with cylinder phantom data and expressed as standardized uptake values (SUV). For the whole-body scans (continuous bed motion acquisition), the radioactivity in the region of interest was estimated by percent of total radioactivity at each frame. After PET scanning, rats were euthanized and perfused with saline. Radioactivity of each tissue type was measured by using a gamma counter (Wallac1470, PerkinElmer, Waltham, MA, USA).

All experimental protocols were approved by the RIKEN Ethics Committee on Animal Care and Use and were performed in accordance with the Principles of Laboratory Animal Care (NIH publication No. 85-23, revised 1985).

Supporting Information: Instrument details, synthetic protocols and characterization data including NMR spectra for compounds **1**–**6** and the radiosynthesis of [^{11}C]-**1** are given in the Supporting Information along with the ex vivo assay procedure for evaluation in GT+FK cells.

Acknowledgements

The authors thank Ms. Tomomi Saeki and Ms. Miku Yamada (Center for Emerging Infectious Diseases, Gifu University) for outstanding research assistance. The authors also thank Dr. Hiroko Koyama (United Graduate School of Drug Discovery and Medical Information Science, Gifu University) for helpful discussion. This work was supported by the Program for the Promotion of Fundamental Studies in Health Sciences of the National Institute of Biomedical Innovation and the Molecular Imaging Research Program of the Ministry of Education, Culture, Sports, Science and Technology of Japan.

Keywords: antiprion agents · brain uptake · positron emission tomography (PET) · prion diseases · radiolabeling

[1] S. B. Prusiner, *Proc. Natl. Acad. Sci. USA* **1998**, *95*, 13363.
[2] S. B. Prusiner, M. R. Scott, S. J. DeArmond, F. E. Cohen, *Cell* **1998**, *93*, 337.
[3] N. R. Cashman, B. Caughey, *Nat. Rev. Drug Discovery* **2004**, *3*, 874.
[4] V. L. Sim, B. Caughey, *Infect. Disord.: Drug Targets* **2009**, *9*, 81.
[5] T. Koster, K. Singh, M. Zimmermann, E. Gruys, *J. Vet. Pharmacol. Ther.* **2003**, *26*, 315.
[6] I. Zerr, *Infect. Disord.: Drug Targets* **2009**, *9*, 92.
[7] J. Hosokawa-Muto, Y. O. Kamatari, H. K. Nakamura, K. Kuwata, *Antimicrob. Agents Chemother.* **2009**, *53*, 765.
[8] T. Kimura, J. Hosokawa-Muto, K. Asami, T. Murai, K. Kuwata, *Eur. J. Med. Chem.* **2011**, *46*, 5675.
[9] K. Kuwata, N. Nishida, T. Matsumoto, Y. O. Kamatari, J. Hosokawa-Muto, K. Kodama, H. K. Nakamura, K. Kimura, M. Kawasaki, Y. Takakura, S. Shirabe, J. Takata, Y. Kataoka, S. Katamine, *Proc. Natl. Acad. Sci. USA* **2007**, *104*, 11921.
[10] N. Yamamoto, K. Kuwata, *J. Phys. Chem. B* **2009**, *113*, 12853.
[11] T. Ishikawa, T. Ishikura, K. Kuwata, *J. Comput. Chem.* **2009**, *30*, 2594.
[12] A. Kranjc, S. Bongarzone, G. Rossetti, X. Biarnés, A. Cavalli, M. L. Bolognesi, M. Roberti, G. Legname, P. Carloni, *J. Chem. Theory Comput.* **2009**, *5*, 2565.
[13] A. J. Nicoll, C. R. Trevitt, M. H. Tattum, E. Risse, E. Quarterman, A. A. Ibarra, C. Wright, G. S. Jackson, R. B. Sessions, M. Farrow, J. P. Waltho, A. R. Clarke, J. Collinge, *Proc. Natl. Acad. Sci. USA* **2010**, *107*, 17610.
[14] T. Kimura, J. Hosokawa-Muto, Y. O. Kamatari, K. Kuwata, *Bioorg. Med. Chem. Lett.* **2011**, *21*, 1502.
[15] J. Hosokawa-Muto, T. Kimura, K. Kuwata, *Drug Chem. Toxicol.* **2012**, *35*, 264.
[16] C. M. Lee, L. Farde, *Trends Pharmacol. Sci.* **2006**, *27*, 310.
[17] O. Milhavet, H. E. M. McMahon, W. Rachidi, N. Nishida, S. Katamine, A. Mangé, M. Arlotto, D. Casanova, J. Riondel, A. Favier, S. Lehmann, *Proc. Natl. Acad. Sci. USA* **2000**, *97*, 13937.
[18] N. Nishida, D. A. Harris, D, Vilette, H. Laude, Y. Frobert, J. Grassi, D. Casanova, O. Milhavet, S. Lehmann, *J. Virol.* **2000**, *74*, 320.
[19] M. Suzuki, H. Koyama, M. Takashima-Hirano, H. Doi in *Positron Emission Tomography: Current Clinical and Research Aspects* (Ed.: C.-H. Hsieh), InTech, Rijeka, **2012**, Chap. 5, pp. 114–152.
[20] M. Suzuki, H. Doi, *J. Synth. Org. Chem. Jpn.* **2010**, *68*, 1195.
[21] M. Suzuki, H. Doi, T. Hosoya, B. Långström, Y. Watanabe, *TrAC Trends Anal. Chem.* **2004**, *23*, 595.
[22] M. Suzuki, R. Noyori, B. Långström, Y. Watanabe, *Bull. Chem. Soc. Jpn.* **2000**, *73*, 1053.

[23] T. Takashima, S. Kitamura, Y. Wada, M. Tanaka, Y. Shigihara, H. Ishii, R. Ijyuin, S. Shiomi, T. Nakae, Y. Watanabe, Y. Cui, H. Doi, M. Suzuki, K. Maeda, H. Kusuhara, Y. Sugiyama, Y. Watanabe, *J. Nucl. Med.* **2012**, *53*, 741.
[24] M. Kosugi, T. Ohya, T. Migita, *Bull. Chem. Soc. Jpn.* **1983**, *56*, 3855.
[25] J. Barluenga, A. M. Bayón, P. Campos, G. Asensio, E. Gonzalez-Nuñez, Y. Molina, *J. Chem. Soc. Perkin Trans. 1* **1988**, 1631.
[26] E. Negishi, *Acc. Chem. Res.* **1982**, *15*, 340.
[27] J. K. Stille, *Angew. Chem.* **1986**, *98*, 504; *Angew. Chem. Int. Ed. Engl.* **1986**, *25*, 508.
[28] P. Espinet, A. M. Echavarren, *Angew. Chem.* **2004**, *116*, 4808; *Angew. Chem. Int. Ed.* **2004**, *43*, 4704.
[29] R. Demaimay, K. T. Adjou, V. Beringue, S. Demart, C. I. Lasmézas, J. P. Deslys, M. Seman, D. Dormont, *J. Virol.* **1997**, *71*, 9685.
[30] K. Doh-ura, K. Ishikawa, I. Murakami-Kubo, K. Sasaki, S. Mohri, R. Race, T. Iwaki, *J. Virol.* **2004**, *78*, 4999.
[31] D. A. Kocisko, W. S. Caughey, R. E. Race, G. Roper, B. Caughey, J. D. Morrey, *Antimicrob. Agents Chemother.* **2006**, *50*, 759.
[32] Y. Tsuboi, K. Doh-Ura, T. Yamada, *Neuropathology* **2009**, *29*, 632.
[33] J. Collinge, M. Gorham, F. Hudson, A. Kennedy, G. Keogh, S. Pal, M. Rossor, P. Rudge, D. Siddique, M. Spyer, D. Thomas, S. Walker, T. Webb, S. Wroe, J. Darbyshire, *Lancet Neurol.* **2009**, *8*, 334.
[34] Y. Huang, H. Okochi, B. C. May, G. Legname, S. B. Prusiner, L. Z. Benet, B. J. Guglielmo, E. T. Lin, *Drug Metab. Dispos.* **2006**, *34*, 1136.
[35] M. Nakajima, T. Yamada, T. Kusuhara, H. Furukawa, M. Takahashi, A. Yamauchi, Y. Kataoka, *Dementia Geriatr. Cognit. Disord.* **2004**, *17*, 158.
[36] K. Doh-ura, K. Tamura, Y. Karube, M. Naito, T. Tsuruo, Y. Kataoka, *Cell. Mol. Neurobiol.* **2007**, *27*, 303.
[37] A. Gallardo-Godoy, J. Gever, K. L. Fife, B. M. Silber, S. B. Prusiner, A. R. Renslo, *J. Med. Chem.* **2011**, *54*, 1010.
[38] A. L. Boxer, G. D. Rabinovici, V. Kepe, J. Goldman, A. J. Furst, S. C. Huang, S. L. Baker, J. P. O'Neil, H. Chui, M. D. Geschwind, G. W. Small, J. R. Barrio, W. Jagust, B. L. Miller, *Neurology* **2007**, *69*, 283.
[39] V. L. Villemagne, C. A. McLean, K. Reardon, A. Boyd, V. Lewis, G. Klug, G. Jones, D. Baxendale, C. L. Masters, C. Rowe, S. J. Collins, *J. Neurol. Neurosurg. Psychiatry* **2009**, *80*, 998.
[40] N. Okamura, Y. Shiga, S. Furumoto, M. Tashiro, Y. Tsuboi, K. Furukawa, K. Yanai, R. Iwata, H. Arai, Y. Kudo, Y. Itoyama, K. Doh-ura, *Eur. J. Nucl. Med. Mol. Imaging* **2010**, *37*, 934.

Received: April 18, 2013
Published online on May 24, 2013

Bioorganic & Medicinal Chemistry 21 (2013) 6378–6384

Contents lists available at ScienceDirect

Bioorganic & Medicinal Chemistry

journal homepage: www.elsevier.com/locate/bmc

Synthesis and structure–activity relationship of 2-phenyliminochromene derivatives as inhibitors for aldo–keto reductase (AKR) 1B10

Satoshi Endo [a,*], Dawei Hu [b], Miho Suyama [a], Toshiyuki Matsunaga [a], Kenji Sugimoto [c], Yuji Matsuya [c], Ossama El-Kabbani [d], Kazuo Kuwata [e], Akira Hara [f], Yukio Kitade [f], Naoki Toyooka [g]

[a] Laboratory of Biochemistry, Gifu Pharmaceutical University, Gifu 501-1196, Japan
[b] Graduate School of Innovative Life Science, University of Toyama, 3190 Gofuku, Toyama 930-8555, Japan
[c] Graduate School of Medicine and Pharmaceutical Sciences, University of Toyama, 2630 Sugitani, Toyama 930-0194, Japan
[d] Monash Institute of Pharmaceutical Sciences, Monash University, Parkville, Victoria 3052, Australia
[e] United Graduate School of Drug Discovery and Medical Information Sciences, Gifu University, Gifu 501-1193, Japan
[f] Department of Biomolecular Science, Faculty of Engineering, Gifu University, Gifu 501-1193, Japan
[g] Graduate School of Science and Technology for Research, University of Toyama, 3190 Gofuku, Toyama 930-8555, Japan

ARTICLE INFO

Article history:
Received 29 July 2013
Revised 23 August 2013
Accepted 23 August 2013
Available online 6 September 2013

Keywords:
AKR1B10
Aldose reductase-like protein
Aldose reductase
Molecular docking
Structure–activity relationship

ABSTRACT

Inhibitors of a human member (AKR1B10) of the aldo–keto reductase superfamily are regarded as promising therapeutics for the treatment of cancer. Recently, we have discovered (*Z*)-2-(4-methoxyphenylimino)-7-hydroxy-*N*-(pyridin-2-yl)-2*H*-chromene-3-carboxamide (**1**) as the potent competitive inhibitor using the virtual screening approach, and proposed its 4-methoxy group on the 2-phenylimino moiety as an essential structural prerequisite for the inhibition. In this study, 18 derivatives of **1** were synthesized and their inhibitory potency against AKR1B10 evaluated. Among them, 7-hydroxy-2-(4-methoxyphenylimino)-2*H*-chromene-3-carboxylic acid benzylamide (**5n**) was the most potent inhibitor showing a K_i value of 1.3 nM. The structure–activity relationship of the derivatives indicated that the 7-hydroxyl group on the chromene ring, but not the 4-methoxy group, was absolutely required for inhibitory activity, The molecular docking of **5n** in AKR1B10 and site-directed mutagenesis of the enzyme residues suggested that the hydrogen-bond interactions between the 7-hydroxyl group of **5n** and the catalytic residues (Tyr49 and His111) of the enzyme, together with a π-stacking interaction of the benzylamide moiety of **5n** with Trp220, are important for the potent inhibition.

1. Introduction

A human member of the aldo–keto reductase (AKR) superfamily, AKR1B10, is a NADPH-dependent reductase, which was originally identified as an aldose reductase-like protein that is up-regulated in hepatocellular carcinomas.[1] Over-expression of AKR1B10 has been also observed in other tumors, such as smokers' non-small cell lung carcinomas,[2] uterine carcinomas,[3] cholangiocarcinomas,[4] pancreatic carcinoma,[5] and breast cancer.[6] The silencing of the AKR1B10 gene results in growth inhibition of cancer cells[5–8] and hepatocellular carcinoma xenografts in mice,[9] and its elevated expression in turn promotes proliferation of cancer cells,[10,11] indicating that the enzyme participates in tumor development. Furthermore, AKR1B10 is suggested to be implicated in developing colon cancer cell resistance to anticancer drugs such as mitomycin C[12] and oxaliplatin.[11] Due to its high catalytic efficiency towards aliphatic aldehydes, retinals and isoprenyl aldehydes,[1,6–8,13,14] the roles suggested for AKR1B10 in cell carcinogenesis and tumor development are the detoxification of cytotoxic carbonyls derived from lipid peroxidation,[6–8] decrease in retinoic acid synthesis,[13] and modulation of protein prenylation.[6,11,15] In addition, AKR1B10 is reported to promote fatty acid synthesis in cancer cells by blocking the ubiquitin-dependent degradation of acetyl CoA carboxylase.[8,16] Thus, this enzyme has been recognized not only as a potential diagnostic and/or prognostic marker, but also as a potential therapeutic target for the treatment of the above types of cancer and the colon cancer chemoresistance.

During the past five years, many synthetic and natural compounds that show inhibitory effects on AKR1B10 have been reported, as reviewed by Matsunaga et al.[11,17] Among them, (*Z*)-2-(4-methoxyphenylimino)-7-hydroxy-*N*-(pyridin-2-yl)-2*H*-chromene-3-carboxamide (**1**) is the most potent competitive inhibitor

Abbreviations: AKR, aldo–keto reductase; FBS, fetal bovine serum; SAR, structure–activity relationship.

* Corresponding author. Tel.: +81 58 237 5979; fax: +81 58 237 3931.
E-mail address: sendo@gifu-pu.ac.jp (S. Endo).

0968-0896/$ - see front matter © 2013 Elsevier Ltd. All rights reserved.
http://dx.doi.org/10.1016/j.bmc.2013.08.059

showing an IC_{50} value of 6.0 nM.[18] Molecular docking of **1** in AKR1B10 proposed that the interactions between the 4-methoxyl group on the 2-phenylimino moiety of **1** and the enzyme's active site residues, His111 and Trp112, are important for the tight binding (Fig. 1A). However, this compound almost equally inhibits the structurally similar human aldose reductase that is named AKR1B1 in the AKR superfamily. Because AKR1B1 plays distinct roles in glucose and prostaglandin metabolism,[19,20] selective inhibition of AKR1B10 is ideally required for the development of drugs targeting this enzyme. The structure–activity relationship (SAR) study on the chromene-3-carboxamide derivatives has not been also reported since its discovery by the virtual screening.[18] In this study, we designed and synthesized derivatives of **1** based on the molecular docking result, and evaluated them for enzyme inhibitory activity, in order to explore SAR of the **1**-derived compounds as potent inhibitors of ARK1B10.

2. Results and discussion

2.1. Chemistry

First, we synthesized seven **1**-based derivatives having different substituents on the 2-phenylimino moiety at the 4-position to confirm the interactions of the 4-methoxy group with His111 and Trp112 of AKR1B10, which was suggested by the previous docking model of **1** in this enzyme.[18] The Knoevenagel condensation of cyanoacetamide (**2**)[21] with 2,4-dihydroxybenzaldehyde (**3**) afforded the 2-iminochromene derivative (**4**). Reaction of **4** with anilines furnished the desired 2-phenyliminochromenes (**5a–g**) (Scheme 1). All of the derivatives potently inhibited AKR1B10, as evidenced by less than 2.2-fold increases in their IC_{50} values compared to that of **1** (See Table 1). Surprisingly, the des-methoxy derivative **5g** also showed potent inhibition, in contrast to the important interaction of the 4-methoxy group suggested by the docking model of **1**.[18] Next, we examined the effect of substituents of the 3-carboxamide moiety on AKR1B10 inhibition. Seven derivatives having isopropyl (**5h**) or acyclic alkyls (**5i–k**), hydroxyalkyls (**5l–m**), and benzyl (**5n**) substituent instead of the 2-pyridyl side chain of **1** were synthesized. Since these substitutions also did not significantly affect the inhibitory potency towards AKR1B10, we synthesized the different phenol derivatives (**5o–q**) and deoxy-derivative (**5r**) at the 7-position of the chromene ring system to examine the role of the 7-hydroxyl group on the chromene ring of **1** and the above derivatives. The same procedures for the synthesis of **5a–g** were applied for the synthesis of **5o–r**, as shown in Schemes 2 and 3.

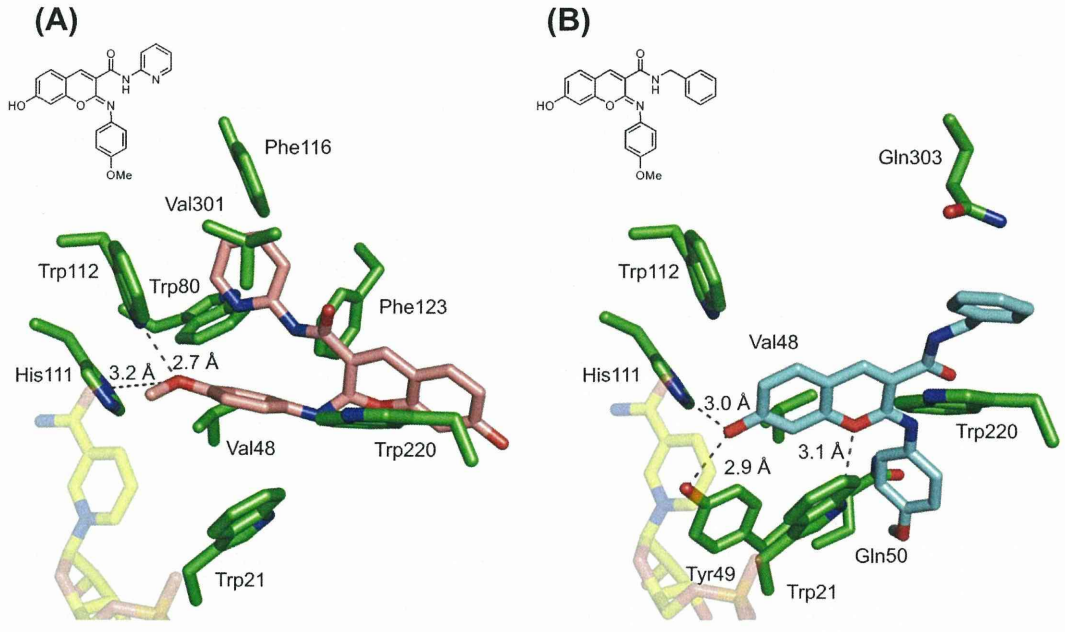

Figure 1. Structures of **1** (A) and **5n** (B), and their docked models in AKR1B10–$NADP^+$ complex. The portion of $NADP^+$ (yellow) and residues (green) within 4.0 Å from the inhibitors are depicted with possible hydrogen bond interactions, which are shown in dotted lines with distances. The docked model of **1** (A) is the same as that previously reported.[18]

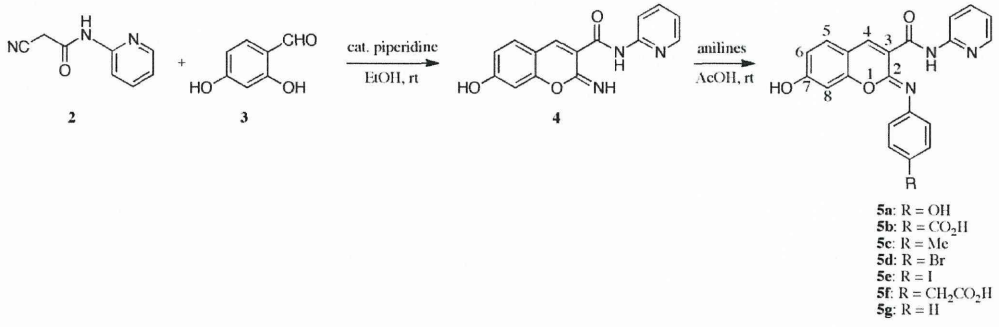

Scheme 1. Synthesis of chromene derivatives **5a–g**.